

Peak effect, plateau effect, and fishtail anomaly: The reentrant amorphization of vortex matter in $2H\text{-NbSe}_2$

S. S. Banerjee,^{1,*} S. Ramakrishnan,¹ A. K. Grover,¹ G. Ravikumar,² P. K. Mishra,² V. C. Sahni,² C. V. Tomy,³ G. Balakrishnan,⁴ D. Mck. Paul,⁴ P. L. Gammel,⁵ D. J. Bishop,⁵ E. Bucher,⁵ M. J. Higgins,⁶ and S. Bhattacharya^{1,6,†}

¹*Department of Condensed Matter Physics and Materials Science, Tata Institute of Fundamental Research, Mumbai-400005, India*

²*Technical Physics and Prototype Engineering Division, Bhabha Atomic Research Centre, Mumbai-400085, India*

³*Department of Physics, Indian Institute of Technology, Powai, Mumbai-400076, India*

⁴*Department of Physics, University of Warwick, Coventry, CV4 7AL, United Kingdom*

⁵*Bell Laboratories, Lucent Technologies, Murray Hill, New Jersey 07974*

⁶*NEC Research Institute, 4 Independence Way, Princeton, New Jersey 08540*

(Received 21 June 1999; revised manuscript received 23 September 1999)

The magnetic field dependence of the critical current is studied in single-crystal samples of the weak pinning type-II superconductor $2H\text{-NbSe}_2$ in the high-temperature and the low-field region of the (H, T) space. The experimental results demonstrate various pinning regimes: a collective pinned quasicrystalline solid in the intermediate-field range that is destabilized in favor of disordered vortex phases in both high fields near H_{c2} and at low fields near H_{c1} . The temperature evolution of the pinning behavior demonstrates how the amorphous limit (where the correlation volume is nearly field independent) is approached around the so-called nose region of the reentrant peak-effect boundary. In the high-field regime the rapid approach to the amorphous limit naturally yields a peak effect, i.e., a peak in the critical current. In the low-field regime the crossover to the individual pinning regime gives rise to a “plateau effect.” We show that with increasing effective pinning the peak effect shifts away from H_{c2} and resembles a “fishtail” anomaly.

I. INTRODUCTION

The role of thermal fluctuations and quenched disorder, i.e., the pinning centers, on the vortex matter in type-II superconductors is a subject of current interest.^{1–5} Enhanced thermal fluctuations cause the melting of an ideal flux line lattice (FLL) into a vortex liquid phase for the high- T_c cuprate (HTSC) systems.^{6,7} At a given temperature, a vortex liquid phase is theoretically expected not only at high fields but also at low fields, i.e., a reentrant liquid phase at low induction.⁸ The pinning centers are expected to add more variety to the above clean system phase diagram in the form of novel pinned vortex phases.^{2–4,9,10} The nature of these phases and the transformations amongst them remain a more controversial subject. In the context of reentrant nature of the FLL melting line, the observation of a reentrant locus of the peak-effect (PE) phenomenon (for dilute flux lines) in the low- T_c superconductor $2H\text{-NbSe}_2$ remains a particularly intriguing result.¹¹ The peak effect phenomenon¹² is the occurrence of an anomalous enhancement of the critical current density, i.e., the pinning force per flux line, at high fields near the normal-state phase boundary (the H_{c2} line) in low- T_c systems and nearly coincident with the melting line in the HTSC's.¹³ The exact causes of the peak effect are uncertain,^{14–16} but it is widely regarded as the result of a rapid softening of the lattice and the occurrence of plastic deformations¹⁴ and proliferation of topological defects^{10,15} in the FLL. The lattice is expected to be amorphous at and above the peak position in J_c .^{10,17}

Recent theoretical work has drawn attention to the possibility of pinning induced glassy phase(s) in the vortex phase diagram.^{2–4} Since the advent of high- T_c era, much of the

experimental efforts have focused on the characteristics of the dense vortex phases,^{9,18,19} for which a different type of critical current density anomaly, termed the fishtail effect (FE) or the second magnetization peak, has been witnessed.⁹ The nomenclature of the FE relates to a characteristic shape of the isothermal dc magnetization hysteresis loop. The FE amounts to a broad maximum in J_c located far away from H_{c2} ; this is in contrast to the conventional PE, which occurs close to H_{c2} . How the two apparently distinct anomalous variations in J_c , the PE and the FE, are related to each other remains a subject of active study.

On the other hand, relatively little is experimentally known about the dilute vortex phases.^{4,20} A recent theoretical picture⁴ proposes that the addition of pinning yields a “reentrant glass” at low densities, analogous to the low-density vortex liquid phase in the pinning-free case.⁸ This raises the question of how the experimentally observed¹¹ reentrance of the peak-effect boundary in NbSe_2 relates to the so-called reentrant liquid⁸ or glassy phase.⁴

In this paper we focus on the magnetic field dependence of the critical current in the high-temperature–low-field region of the (H, T) space in single-crystal samples of $2H\text{-NbSe}_2$. We show explicitly how the pinning evolves from a regime of individual pinning or small bundle pinning to the more collective pinning regime with varying H and T . We track their evolution in samples with different amounts of quenched random disorder and also by exploiting the intrinsic anisotropy of the hexagonal system $2H\text{-NbSe}_2$. These results provide a scenario that mimics the evolution of the characteristics of the critical current density with increasing effective pinning, as reported in the cuprates in the low-temperature–high-field region^{18,19} and in an $A\text{-15}$

superconductor,¹⁹ when the quenched disorder was increased externally. The results in $2H\text{-NbSe}_2$ crystals also explicitly show the nature of a disordering process of the FLL at low fields, which we now propose is actually better described as a “plateau effect” that occurs more conspicuously in more strongly pinned samples. In addition, these results also delineate the regime where a collectively pinned ordered vortex phase exists and specifically bring out how an amorphous phase *surrounds* and/or *swamps* this ordered regime around the so-called “nose” of the peak-effect boundary.¹¹

II. EXPERIMENT

We have extracted the field dependence of critical current density $J_c(H)$ (for $H\parallel c$) in two types of single crystals of $2H\text{-NbSe}_2$ [to be designated as X (Ref. 14) and Y (Ref. 10), respectively] either by directly relating $J_c(H)$ to the width of the isothermal magnetization loop or by analyzing the in-phase and out-of-phase ac susceptibility data²¹ within the framework of the critical state model.^{22,23} The isothermal dc magnetization hysteresis measurements were performed on a commercial quantum design superconducting quantum-interference device (SQUID) magnetometer with a 2 cm full scan length and/or a 4 cm “half-scan technique” prescribed by Ravikumar *et al.*,²⁴ whereas the in-phase and out-of-phase ac susceptibility data with different ac amplitudes were measured using a home-built system. The crystal piece X (dimensions $4 \times 1.74 \times 0.18$ mm³) with $T_c(0) \approx 7.22$ K and resistivity ratio $R_{300\text{ K}}/R_{8\text{ K}}$ of 20 is similar to the one utilized by Higgins and Bhattacharya¹⁴ in their electrical transport experiments. The sample Y (dimensions $5 \times 2 \times 0.2$ mm³) with $T_c(0) \approx 7.17$ K and with resistivity ratio $R_{300\text{ K}}/R_{8\text{ K}}$ of 16 (Ref. 11) is slightly more strongly pinned than crystal X. However, the locus of peak temperatures $T_p(H)$ in this specific sample shows a reentrant characteristic^{11,21} below a field value of 150 Oe at a reduced temperature [$t = T/T_c(0)$] of about 0.98 in the “nose” region. We have verified that there is a satisfactory agreement between the J_c values (at low fields and close to the nose temperature region) estimated from the width of the dc magnetization hysteresis data and those estimated from an analysis of in-phase and out-of-phase ac susceptibility data.^{18,19,22} A simple way to estimate J_c from the in-phase ac susceptibility data²¹ is the generalized critical-state model relationship:²²

$$\chi' \sim -1 + \frac{\alpha h_{ac}}{J_c(H)}. \quad (1)$$

In this relation, α is a geometrical factor that depends upon the size, shape, and orientation of a given specimen with respect to the applied field H . It can be determined for each circumstance by comparing estimates of $J_c(H)$ by different procedures and/or directly measured values of transport $J_c(H, T)$. Note that a small uncertainty in the absolute values of critical current densities in different crystals does not influence the primary objective of the present paper, in which we shall attempt to bring out the characteristic features in the evolution of pinning behavior in different circumstances by examining the *normalized values* of current density. In the field-temperature region of our present interest, $J_c(H, T)$ values in crystal X are in the range of 10^4 – 10^6 A/m², whereas

those in the crystal Y are about five times larger. The resulting values of the ratio of $J_c(H, T)$ to $J_0(T)$, the latter being the depairing current density, are in the range 10^{-4} – 10^{-3} , which confirm the weak pinning status of the crystals under investigations.

In addition, we have utilized the anisotropy of the hexagonal $2H\text{-NbSe}_2$ by examining the changes in the characteristics of magnetization hysteresis loops as the applied field orients away from the c axis of the crystal. For such an angular dependence study, we utilized a larger sized crystal (dimensions $5 \times 4 \times 0.45$ mm³) with $T_c(0) \approx 7.25$ K. At low fields ($H < 200$ Oe) and high temperatures, i.e., for $0.96 < T/T_c(0) < 1$, the locus of $t_p(H)$ [$= T_p(H)/T_c(0)$] values (for $H\parallel c$) in this sample (designated Y') displays behavior similar to that being reported in the crystal Y.

III. RESULTS AND DISCUSSION

A. Isothermal critical current density $J_c(H)$ for $H\parallel c$

Figure 1 summarizes the J_c vs H data ($H\parallel c$) for the crystals X and Y in two sets of log-log plots in the temperature regions close to the respective $T_c(0)$ values. The peaks in $J_c(H)$ occur at fields (H_p) less than 1 kOe [see insets in Figs. 1(c) and 1(g) for $t_p(H)$ curves in X and Y, respectively].

We first focus on the shapes of the $J_c(H)$ curves [cf. Figs. 1(a)–1(d)] in the cleanest crystal X. In Fig. 1(a), the three regimes (marked I, II, and III in the figure) of $J_c(H)$, at a reduced temperature $t \approx 0.973$, can be summarized as follows: (1) At the lowest fields ($H \sim 10$ Oe), J_c varies weakly with field (region I), as expected in individual pinning or small bundle pinning regime, noted earlier also by Duarte *et al.*²⁵ and Marchevsky.²⁶ (2) Above a threshold field value, marked by an arrow, $J_c(H)$ variation (in region II) closely follows the archetypal collective pinning power-law²⁵ dependence ($\sim 1/H$). (3) This power-law regime terminates at the onset (marked by another arrow) position of the peak-effect phenomenon (region III). On increasing the temperature [see Figs. 1(a) and 1(b) for the data at $t = 0.973$ and 0.994 , respectively], the following trends are immediately apparent: (1) The peak effect becomes progressively shallower, i.e., the ratio of $J_c(H)$ at the peak position to that at the onset of the PE becomes smaller. For instance, the ratio has a value of about 8 at $t = 0.973$ and it reduces to a value of 3.5 at $t = 0.994$. (2) The power-law region shrinks. For example, the field interval between the pair of arrows (identifying the power-law region) spans from 10 Oe to about 500 Oe at $t = 0.973$ in Fig. 1(a), whereas at $t = 0.996$ in Fig. 1(c), the power-law regime terminates near 40 Oe. Also, the slope value of linear variation of $\log_{10} J_c$ vs $\log_{10} H$ in the latter case is somewhat smaller. At still higher temperatures [see, for instance, Fig. 1(d) at 0.997], the power-law region is nearly invisible and the anomalous PE peak cannot be distinctly identified anymore, as only a residual shoulder survives.

In contrast, the second set of plots [see Figs. 1(e)–1(h)] in the crystal Y show a somewhat different behavior, although the overall evolution in the shapes of $J_c(H)$ curves is generically the same. In Fig. 1(e), at a reduced temperature $t \approx 0.965$, one can see the same power-law regime as in Fig.

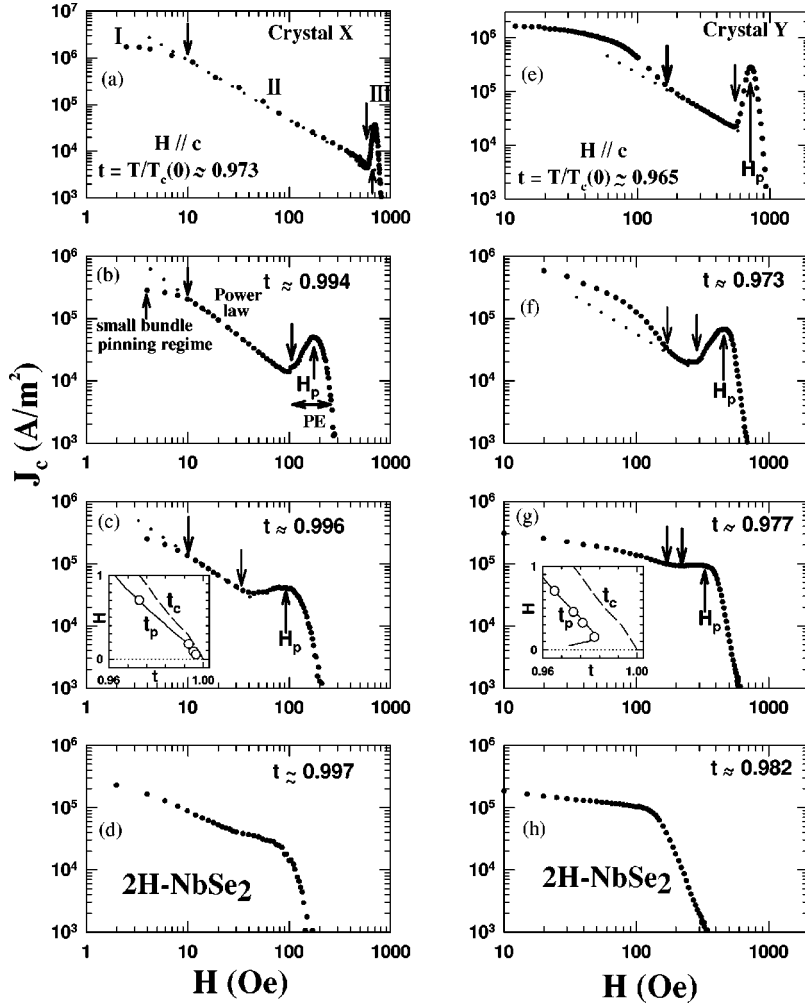


FIG. 1. Log-log plots of J_c vs $H(\parallel c)$ at selected temperatures in crystals X and Y of $2H\text{-NbSe}_2$. The three different pinning regimes (I, II, and III) have been identified at $t=0.973$ in crystal X in (a). The insets in (c) and (g) display the PE curve $t_p(H) [=T_p(H)/T_c(0)]$ and the superconductor-normal phase boundary $t_c(H) [=T_c(H)/T_c(0)]$ in crystals X and Y, respectively (Ref. 11). The marked data points on the PE curves in each of these insets identify the reduced temperatures at which $J_c(H)$ data have been displayed in (a)–(d) and in (e)–(h). The $J_c(H)$ plot at $t=0.997$ in crystal X in (d) and that at $t=0.982$ in crystal Y in (h) show that the peak effect cannot be identified distinctly at the corresponding temperatures. Note the location of these two reduced temperature values in the insets of (c) and (g), respectively; they lie near the ‘‘nose’’ region of the respective $t_p(H)$ curves.

1(a), but as the extrapolated dotted line shows, $J_c(H)$ departs from the power-law behavior in the low-field region (i.e., for $H < 200$ Oe). As the field decreases below 200 Oe, the current density in crystal Y ($t=0.965$) starts to increase more rapidly (than that given by the power law) towards the background saturation limit (i.e., the current density at the lower field end). As compared to the crystal Y, the approach to background saturation limit occurs at a much lower field ($H < 10$ Oe) in crystal X. The smooth crossover to individual or small bundle pinning regime, as seen in crystal X, has therefore added on an additional characteristic in the crystal Y. Further, with increasing temperature, the power-law regime in crystal Y shrinks faster than that in sample X [cf. Fig. 1(e) at $t=0.965$ and Fig. 1(f) at $t=0.973$], leaving only a rather featureless monotonic $J_c(H)$ behavior up to the highest fields [cf. Figs. 1(g) and 1(h)]. Note also that the limiting value of the reduced temperature up to which the power-law regime along with the PE peak survives in crystal Y is smaller than that in crystal X. In crystal Y, the PE peak can be distinctly discerned only up to $t=0.977$, whereas in crystal X it can be seen even up to $t=0.994$. Recalling that crystal Y is more strongly pinned than crystal X, the above observation reaffirms the notion¹¹ that the progressive enhancement in effective pinning (which occurs as we go from sample X to Y) shrinks the (H, T) region over which the vortex matter responds like an elastically pinned vortex lattice.

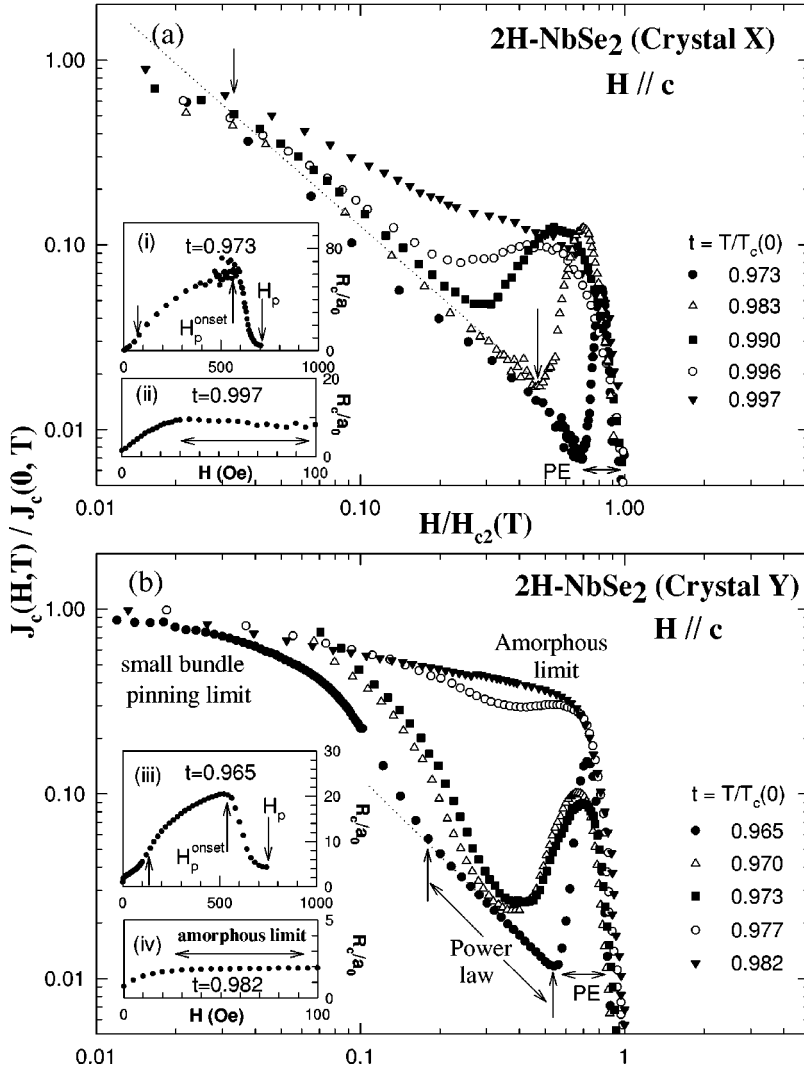
B. Evolution in pinning characteristic through plots of $J_c(b)$

Küpfer *et al.*¹⁹ had drawn attention to the evolution in pinning behavior in weakly pinned crystals of $\text{YBa}_2\text{Cu}_3\text{O}_{7-\delta}$ and V_3Si via plots of current density versus normalized field H/H_{irr} , where H_{irr} is the irreversibility field (as $H \rightarrow H_{irr}$, $J_c \rightarrow 0$). In analogy with this work, we consider it instructive to view plots of normalized values of current density $J_c(H)/J_c(H=0)$ versus reduced field $b (=H/H_{c2})$ at different temperatures in our crystals of NbSe_2 . In these crystals, the peak effect and the irreversibility line are located very close to the upper critical field [$H_{c2}(T)$] line. In view of the fact that $J_c(H=0)$ increases as temperature decreases, the normalization of $J_c(H)$ by $J_c(0)$ implicitly takes into account the overall effect of the change in temperature. Another motivation for plotting the current density versus b stems from the dependence of shear (c_{66}) and tilt (c_{44}) elastic moduli of triangular FLL on the reduced field at a given temperature.^{12,27,28} The competition between elasticity of the FLL and pinning governs the correlation volume V_c of the Larkin domain, which relates inversely to J_c as²⁷

$$HJ_c \sim \sqrt{\frac{nf^2}{V_c}}, \quad (2)$$

where n is the density of pins and f represents the strength of elementary pinning interaction.

Fig.2 (S. S. Banerjee et al)



Figures 2(a) and 2(b) show the resulting plots of $J_c(H)/J_c(0)$ in crystals X and Y of $2H\text{-NbSe}_2$ at selected temperatures. The evolution of $J_c(H)$ curves in these two sets of plots and its commonality with similar sets of plots in the cases of cuprate superconductor $\text{YBa}_2\text{Cu}_3\text{O}_{7-\delta}$ (Refs. 18 and 19) and the A15 alloy V_3Si (Ref. 19) now become very apparent. Note first, that in crystal X [see Fig. 2(a)], the departure from the collective pinning behavior occurs at smaller values of the reduced field as the temperature increases. For example, in Fig. 2(a) at $t=0.973$, the departure from the power-law response occurs around $b=0.71$, while at $t=0.996$, this departure occurs at $b=0.134$. At the highest temperatures (for instance, $t=0.996$ and $t=0.997$), the conventional sharp peak effect evolves into a broad hump away from the corresponding H_{c2} value [cf. Fig. 2(a) and Fig. 1(d)], reminiscent of the FE. The evolution of $J_c(H)$ curves from the PE to the FE in crystals of $\text{YBa}_2\text{Cu}_3\text{O}_{7-\delta}$ and V_3Si has been reported to occur either by progressive increase in pinning centers¹⁹ or by progressive decrease in temperature for a given amount of δ in $\text{YBa}_2\text{Cu}_3\text{O}_{7-\delta}$,^{18,19} in marked contrast to that by the increase in temperature as in the present case of NbSe_2 . It is nevertheless reasonable to suggest that the vortex matter becomes amorphous in the field region of the broad hump, and consequently the correlation

FIG. 2. Log-log plots of $J_c(H)/J_c(0)$ vs $H/H_{c2}(T)$ for $H \parallel c$ at selected temperatures in crystals X and Y of $2H\text{-NbSe}_2$. The PE region has been identified at the lowest reduced temperature for crystals X and Y in (a) and in (b), respectively. The normalized current density reaches up to a limiting value at the peak of the PE. This limiting value is marked as the amorphous limit in (b). The insets (i) and (ii) in (a) and insets (iii) and (iv) in (b) show R_c/a_0 vs H at two sets of reduced temperatures in crystals X and Y, respectively. The amorphous limit of R_c/a_0 , which corresponds to its field-independent value at a high temperature ($t=0.982$ in crystal Y), has been identified in the inset (iv) of (b). Note that R_c/a_0 at $H=H_p$ in the inset (i) in (a) and in inset (iii) in (b) reaches the respective field-independent limiting value (see text for details).

volume V_c does not vary significantly in this region. Thus, in such a regime [e.g., curves at $t=0.997$ and $t=0.982$ in Figs. 2(a) and 2(b), respectively] the pinning is expected to track the field dependence of the elementary pinning interaction f in Eq. (2). It is pertinent to point out here that at temperatures, where the PE is very pronounced, $J_c(H)$ rises from its smallest value in the collective pinning regime at the onset of the PE to reach its overall amorphous limit at the peak position [cf. curves from $t=0.973$ to 0.990 in Fig. 2(a) and those from $t=0.965$ to 0.973 in Fig. 2(b)], as proposed in the original Larkin-Ovchinnikov (LO) scenario.²⁷ The $J_c(H)$ curves for the more strongly pinned crystal Y approach the individual pinning limit faster than those in crystal X [compare curves at $t=0.965$ to 0.982 in Fig. 2(b) with those at $t=0.973$ and 0.983 in Fig. 2(a)].

The above description leads us to propose that at a given temperature, the entire field span is subdivided into three primary pinning regimes: the single-particle or small-bundle regime at low fields, a collective pinning of an ordered lattice regime at intermediate fields, and finally the departure back to a single-particle or amorphous regime at high fields [as marked by arrow at the onset of the PE in Figs. 2(a) and 2(b)]. It is also obvious that the vortex system fails to reach the intermediate regimes of the collectively pinned ordered lattice at high temperatures very close to $T_c(0)$.

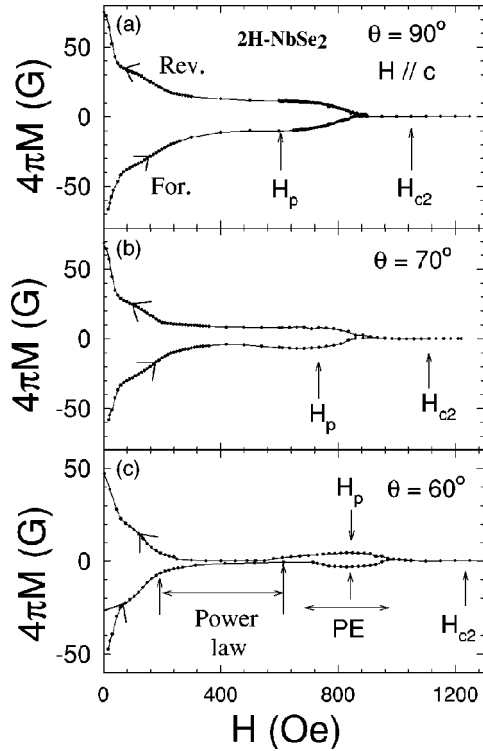


FIG. 3. The panels (a) to (c) show the portions of the forward ($-H_{max}$ to $+H_{max}$) and the reverse ($+H_{max}$ to $-H_{max}$) magnetization hysteresis curves at $T=7.0$ K at three orientations of the crystal Y' of NbSe_2 .

C. Angular dependence of critical current density and its relationship with evolution in pinning behavior

The evolution of pinning crossovers in $2H\text{-NbSe}_2$ system can also be elucidated by examining the changes in the shape of the magnetization hysteresis loop as the c axis of the single crystal orients away from the direction of the applied field. In such a circumstance, the thermal energy remains fixed, but the field span over which the effects of interaction (leading to collective pinning regime) can dominate expands as a consequence of an increase in H_{c2} , following the anisotropic Ginzburg-Landau formalism relationship:

$$H_{c2} = H_{c2}(\parallel c, T) [\sin^2(\theta) + \epsilon^2 \cos^2(\theta)]^{-1/2}, \quad (3)$$

where $\epsilon = H_{c2}(\parallel c)/H_{c2}(\parallel ab)$ and θ is the angle between the applied field H and the ab plane of the single crystal of NbSe_2 .^{1,14} As θ changes from $\pi/2$ towards 0, H_{c2} increases from $H_{c2}(\parallel c, T)$ to $H_{c2}(\parallel ab, T)$, and simultaneously the peak field $H_p(\theta)$ also increases as the ratio $H_p(\theta)/H_{c2}(\theta)$ remains nearly invariant.¹⁴ The increase in the peak field in turn also implies that the field span over which the collective pinning power law behavior holds would expand. For instance, Figs. 3(a)–3(c) display M - H loops from $\theta = \pi/2$ to $\theta = \pi/3$ at $T=7.0$ K in crystal Y' of $2H\text{-NbSe}_2$. Note the qualitative difference in the shapes of the two loops in Figs. 3(a) and 3(c). Its significance could become apparent from the plots of normalized values of hysteresis width versus respective reduced fields.

Figure 4 summarizes the angular dependence of the normalized magnetization data as log-log plots, following the prescription of Fig. 2. It is apparent that in the M - H loop for

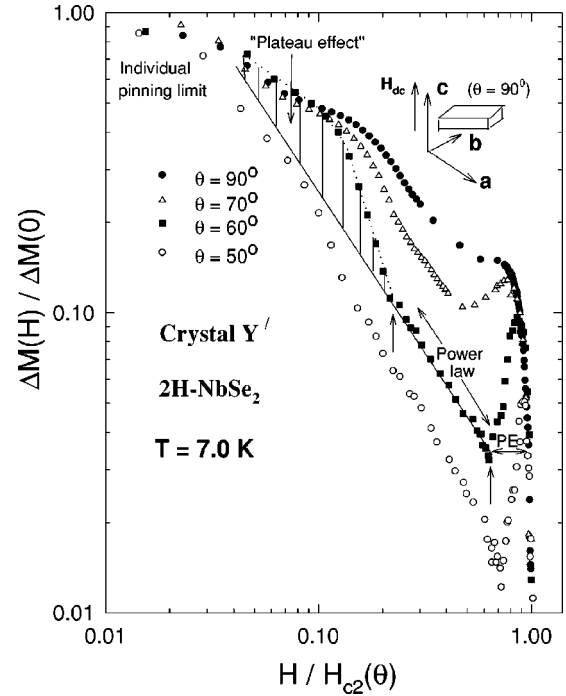


FIG. 4. Display of the normalized values of the width of magnetization hysteresis loop vs $H/H_{c2}(\theta)$ on a log-log plot for various values of θ . In the curve corresponding to $\theta=60^\circ$ ($\pi/3$), the two arrows mark the power-law regime. The extrapolated solid line passing through the data points in the power-law regime and the dotted line passing through the data point in the field region below the lower limit of the power-law regime demonstrates the surfacing of the low field anomaly, i.e., the *plateau effect* phenomenon.

$H\parallel c$ at 7 K [see Fig. 3(a)], the collective pinning power-law regime sandwiched between the individual pinning limit at the low-field end and the amorphous limit near the H_{c2} end cannot be distinctly delineated. This M - H loop reminds us of the *fishtail effect*. However, as the angle θ reaches $\pi/3$ [see the evolution of behavior in Fig. 4 and the M - H loop in Fig. 3(c)], the three regimes can be easily identified. These correspond to the conventional peak effect near H_{c2} , the interaction-dominated collective pinning power-law region at intermediate fields, and the pinning-induced rapid approach to the individual pinning limit at low fields (which accounts for the reentrant characteristic in the PE curve). The solid line and the dashed line drawn for the curve at $\theta = \pi/3$ in Fig. 4 help to focus on a *reverse* amorphization process as the vortex matter enters the dilute regime [FLL constant a_0 of 3500 \AA at $H \approx 200$ Oe exceeds the penetration depth λ_{ab} of 3000 \AA at $t=0.97$ (Ref. 29)] from the ordered elastic vortex solid regime while decreasing the field. At this juncture, it is tempting to draw an analogy between the Gingras and Huse⁴ scenario (of an elastically deformed pinned vortex lattice state sandwiched between the higher-density vortex glass phase and the very-low-density “reentrant glass” state) and our experimental observation of a collectively pinned quasiordered vortex state sandwiched between a highly concentrated amorphous vortex state and a very dilute disordered vortex array in the (nearly) individual pinning regime. To reiterate the crossover from collective pinning regime to each of the other two regimes results in an anomalous increase in J_c values. In the case of the upper PE anomaly, the

$J_c(H)$ rapidly declines from the peak position of the PE due to a collapse of the strength f of individual pins [cf. Eq. (2)] while approaching the normal state. On the other hand, in the case of the *reverse* anomaly, from the position of the hump (see, for instance, the shaded portion in Fig. 4 corresponding to the curve for $\theta = \pi/3$), the $J_c(H)$ values smoothly cross over and approach the individual pinning limit. Therefore, we propose that the crossover to an individual pinning limit (i.e., reverse anomaly) is better termed the ‘‘plateau effect.’’

D. Estimation of correlation lengths

The volume V_c of a Larkin domain within which vortices remain well correlated is usually written as, $V_c = R_c^2 L_c$, where R_c and L_c are radial and longitudinal correlation lengths for the flux line lattice. Once $J_c(H)$ is determined in a crystal to which the LO (Ref. 27) collective pinning description applies, the correlation lengths, R_c and L_c , can in principle be computed [see Eq. (2)] as L_c and R_c are related to each other through the ratio of elastic moduli c_{44} and c_{66} .^{12,27}

It is useful to view [see insets (i) and (ii) in Figs. 2(a) and insets (iii) and (iv) in Fig. 2(b)] the computations of R_c vs H in crystals X and Y at temperatures corresponding to the two extreme behaviors of current density data in the main panels of Figs. 2(a) and 2(b). These computations have been made using respective $J_c(H)$ values in crystals X and Y and following the two- and three-dimensional (2D and 3D) collective pinning analysis made by Angurel *et al.*²³ as per their Eqs. (7) and (8). It was surmised by them²³ and we have confirmed²⁹ by estimating the longitudinal correlation length L_c from $J_c(0)$ data in crystal X (Ref. 14) that the 2D collective pinning description (for which $L_c >$ thickness of the sample) is more appropriate for crystal X. On the other hand, our estimates of L_c show²⁹ that the 3D collective pinning scenario prevails in crystal Y. The analysis indeed finds [cf. data in insets in Figs. 2(a) and 2(b)] that the values of the ratio R_c/a_0 in crystal X at $t = 0.983$ are larger than those in the more strongly pinned crystal Y at a comparable value of t . The R_c/a_0 values in crystals X and Y also appear reasonable in the context of estimates of R_c/a_0 reported by Angurel *et al.*²³ in much more strongly pinned crystals of $2H\text{-NbSe}_2$. We note further that the ratio of R_c/a_0 starts to collapse at H_p^{onset} [see inset (i) in Fig. 2(a) as well as inset (iii) in Fig. 2(b)], and at the peak field H_p , it approaches the amorphous limit as given by its estimate shown in inset (ii) in Fig. 2(a) or inset (iv) in Fig. 2(b). Note that in inset (i) in Fig. 2(a), $R_c/a_0 \sim 2$ at $H = H_p$ for crystal Y, whereas $R_c/a_0 \sim 5$ at $H = H_p$ in crystal X in inset (iii) in Fig. 2(b); these estimates are at present just at an order of magnitude level. They are based on a collective pinning prescription whose validity between the onset and peak positions of the PE still remains to be established. The central observation is that in a given sample, the current density at $H = H_p$ is of the same order as the current density in the amorphous limit, i.e., when $J_c(H)$ is nearly field independent far below H_{c2} and does not display a collective pinning power-law behavior as at $t = 0.997$ in sample X and at $t = 0.982$ in sample Y.

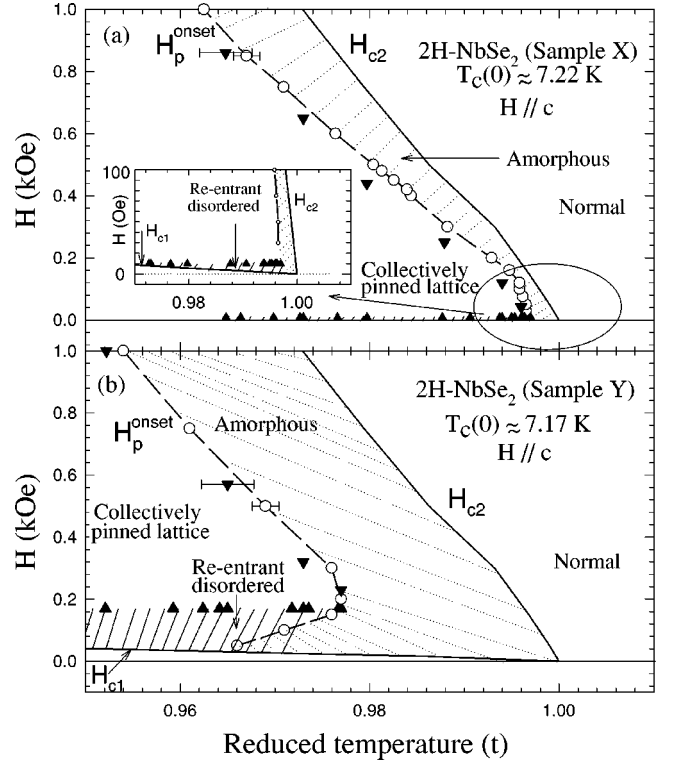


FIG. 5. Vortex phase diagrams in the low-field–high-temperature (i.e., $H < 1$ kOe and $0.95 < T/T_c(0) < 1.0$) region in crystals X and Y of $2H\text{-NbSe}_2$. The region between the onset of conventional peak effect phenomenon (H_p^{onset}) and the superconductor-normal phase boundary (H_{c2}) has been filled with dotted lines, whereas the low-field region below the start of power-law behavior in $J_c(H)$ (see Fig. 1) has been shaded with solid lines. The filled triangle data points identify the limiting fields above which power-law behavior prevails [see, for instance, Figs. 1(a) and 1(b)]. Note that the collectively pinned quasiordered lattice region appears sandwiched between the so-called reentrant disordered region and the amorphous region for $0.97 < t < 0.995$ in crystal X in (a) and for $0.96 < t < 0.98$ in crystal Y in (b). The curves H_p^{onset} in (a) and (b) correspond to the temperatures of the onset of the peak effect in isofield $\chi'_{ac}(T)$ scans as reported by Banerjee *et al.* in Ref. 11. The filled inverted triangle data points identify the fields corresponding to the upper ends of collectively pinned power-law behavior as shown in Figs. 1(a)–1(c) and 1(e)–1(g) for samples X and Y, respectively. Note that such fields are consistent with the respective H_p^{onset} lines, keeping in view the probable error bars on each of the data points. For the sake of completeness, the lower critical field $H_{c1}(T)$ line (Ref. 11) has also been drawn in each of the phase diagrams.

IV. CONSTRUCTION OF THE VORTEX PHASE DIAGRAM

It is instructive to collate in Fig. 5 the domains of a collectively pinned ordered state (cf. power-law regimes in Figs. 1 and 2) as distinct from the high-field conventional PE region and the low-field individual pinning limit (i.e., the plateau effect) region in crystals X and Y of $2H\text{-NbSe}_2$. In the magnetic phase diagrams shown in Figs. 5(a) and 5(b), the field-temperature region between the start of the PE and the $H_{c2}(T)$ line has been filled with dotted lines and termed as *amorphous* region, whereas the lower field (individual) pinning-dominated region has been shaded with solid lines and termed as *reentrant disordered*. The so-called *amorphous* and *reentrant disordered* regions overlap and form a

continuum in the neighborhood of the nose region of the PE curve [recall $t_p(H)$ curves in the insets of Figs. 1(c) and 1(g)]. Thus, the phase diagrams in Figs. 5(a) and 5(b) further clarify how the enhancement in quenched random inhomogeneities, as measured by the increase in J_c values, shrinks the domain of the collectively pinned and the elastically deformed ordered state in the field-temperature region where the interplay between thermal fluctuations and pinning effects predominates. At temperatures above the nose region, the combination of the thermal fluctuations and the pinning centers destabilizes the ordered lattice over the entire field regime.

V. CONCLUSION

To conclude, we have demonstrated the evolution of the pinning behavior through the isothermal $J_c(H)$ in the high-temperature part of the (H, T) phase diagram in weak pinning samples of $2H\text{-NbSe}_2$. The results show that the collectively pinned vortex solid (presumably akin to a Bragg glass²) is destabilized at both high and low fields. At high fields, the critical current increases rapidly to merge with the amorphous limit, and it then decreases rapidly with further increase in H due primarily to the collapse of the pinning parameter f in Eq. (2), resulting in a conventional peak effect. At higher temperatures, the peak effect moves away from H_{c2} in the reduced (temperature/field) scale and becomes a broader anomaly, strongly resembling a fishtail effect. At low fields, on the other hand, the critical current increases rapidly to merge with the amorphous limit which, by contrast, is a weakly-field-dependent individual pinning regime and we have designated this as a plateau effect. In

some circumstances, all these effects can be identified as distinct features lying in juxtaposition to each other, whereas in others they are admixed in a manner that the regime of stability of an ordered vortex lattice becomes obscure. The latter kind of behavior has often been reported in recent years in a variety of HTSC's over a very wide field-temperature span unlike in $2H\text{-NbSe}_2$ where such a behavior is seen in a very limited field-temperature region near $T_c(0)$.

Both the peak effect and the plateau effect mark an amorphization of vortex matter at the high-field and low-field limits, respectively. The resulting "phase diagram" of different pinning behavior elucidates the details of the reentrance phenomenon of the peak effect observed earlier¹¹ in constant H and varying T measurements. We caution that the line(s) drawn in Fig. 5 imply a change in pinning regime (across such a boundary).^{1,18} Whether they also represent thermodynamic transformations cannot be determined from the measurements reported here. Further work is needed to settle this issue. Finally, we note that Paltiel *et al.*³⁰ have drawn attention to the importance of surface barriers at low fields in crystals of $2H\text{-NbSe}_2$. In the field-temperature region of our present work, the shape of the M - H loops (see, for instance, Fig. 3) suggests that the surface barrier effects are not prominent.

ACKNOWLEDGMENTS

We would like to acknowledge Nandini Trivedi, Satya Majumder, and Mahesh Chandran for fruitful discussions. The work at Warwick University is supported by a research grant from EPSRC, U.K.

*Email address: sb@mailhost.tifr.res.in

†Email address: shobo@research.nj.nec.com

¹G. Blatter, M. V. Feigel'man, V. B. Geshkenbein, A. I. Larkin, and V. M. Vinokur, *Rev. Mod. Phys.* **66**, 1125 (1994), and references therein.

²T. Giamarchi and P. Le Doussal, *Phys. Rev. Lett.* **72**, 1530 (1994); *Phys. Rev. B* **52**, 1242 (1995), and references therein.

³D. S. Fisher, M. P. A. Fisher, and D. A. Huse, *Phys. Rev. B* **43**, 130 (1991).

⁴M. Gingras and D. A. Huse, *Phys. Rev. B* **53**, 15 193 (1996).

⁵T. Giamarchi and P. Le Doussal, *Phys. Rev. Lett.* **76**, 3408 (1996); *Phys. Rev. B* **57**, 11 356 (1996).

⁶E. Zeldov, D. Majer, M. Konczykowski, V. M. Vinokur, and H. Shtrikman, *Nature (London)* **375**, 373 (1995).

⁷A. Schilling, R. A. Fisher, N. E. Phillips, U. Welp, D. Dasgupta, W. K. Kwok, and G. W. Crabtree, *Nature (London)* **382**, 791 (1996).

⁸D. R. Nelson, *Phys. Rev. Lett.* **60**, 1973 (1988).

⁹M. Daeumling, J. M. Seuntjens, and D. C. Larbalestier, *Nature (London)* **346**, 332 (1990); M. Werner, F. M. Sauerzopf, H. W. Weber, B. W. Veal, F. Licci, K. Winzer, and M. R. Koblischka, *Physica C* **235-240**, 2833 (1994); M. F. Goffman, J. A. Herb-sommer, F. de la Cruz, T. W. Li, and P. H. Kes, *Phys. Rev. B* **57**, 3663 (1998), and references therein.

¹⁰S. S. Banerjee, N. G. Patil, S. Saha, S. Ramakrishnan, A. K. Grover, S. Bhattacharya, G. Ravikumar, P. K. Mishra, T. V. Chandrasekhar Rao, V. C. Sahni, M. J. Higgins, E. Yamamoto,

Y. Haga, M. Hedo, Y. Inada, and Y. Onuki, *Phys. Rev. B* **58**, 995 (1998); S. S. Banerjee, N. G. Patil, S. Ramakrishnan, A. K. Grover, S. Bhattacharya, G. Ravikumar, P. K. Mishra, T. V. Chandrasekhar Rao, V. C. Sahni, M. J. Higgins, C. V. Tomy, G. Balakrishnan, and D. Mck. Paul, *ibid.* **59**, 6043 (1999).

¹¹K. Ghosh, S. Ramakrishnan, A. K. Grover, Gautam I. Menon, Girish Chandra, T. V. Chandrasekhar Rao, G. Ravikumar, P. K. Mishra, V. C. Sahni, C. V. Tomy, G. Balakrishnan, D. Mck. Paul, and S. Bhattacharya, *Phys. Rev. Lett.* **76**, 4600 (1996); S. S. Banerjee, N. G. Patil, S. Ramakrishnan, A. K. Grover, S. Bhattacharya, G. Ravikumar, P. K. Mishra, T. V. Chandrasekhar Rao, V. C. Sahni, M. J. Higgins, C. V. Tomy, G. Balakrishnan, and D. Mck. Paul, *Europhys. Lett.* **44**, 91 (1998).

¹²M. Tinkham, *Introduction to Superconductivity*, 2nd ed. (McGraw-Hill, New York, 1996), Chap. 9.

¹³K. Kwok, J. A. Feudrich, C. J. Van der Beck, and C. W. Crabtree, *Phys. Rev. Lett.* **73**, 2614 (1994).

¹⁴S. Bhattacharya and M. J. Higgins, *Phys. Rev. Lett.* **70**, 2617 (1993); M. J. Higgins and S. Bhattacharya, *Physica C* **257**, 232 (1996) and references therein.

¹⁵C. Tang, X. Ling, S. Bhattacharya, and P. M. Chaikin, *Europhys. Lett.* **35**, 597 (1996), and references therein.

¹⁶A. I. Larkin, M. C. Marchetti, and V. M. Vinokur, *Phys. Rev. Lett.* **75**, 2992 (1995).

¹⁷P. L. Gammel, U. Yaron, A. P. Ramirez, D. J. Bishop, A. M. Chang, R. Ruel, L. N. Pfeiffer, and E. Bucher, *Phys. Rev. Lett.* **80**, 833 (1998).

- ¹⁸T. Nishizaki, T. Naito, and N. Kobayashi, *Phys. Rev. B* **58**, 11 169 (1998).
- ¹⁹H. Küpfer, Th. Wolf, C. Lessing, A. A. Zhukov, X. Lanon, R. Meier-Hirmer, W. Schauer, and H. Wuehl, *Phys. Rev. B* **58**, 2886 (1998), and references cited therein.
- ²⁰D. R. Nelson and P. Le Doussal, *Phys. Rev. B* **42**, 10 113 (1990); S. Ryu, S. Doniach, G. Deutscher, and A. Kapitulnik, *Phys. Rev. Lett.* **68**, 710 (1992); M. I. J. Probert and A. I. M. Rae, *ibid.* **75**, 1835 (1995); G. Blatter and V. Geshkenbein, *ibid.* **77**, 4958 (1996).
- ²¹S. Ramakrishnan, K. Ghosh, A. K. Grover, Gautam I. Menon, Girish Chandra, T. V. Chandrasekhar Rao, P. K. Mishra, G. Ravikumar, V. C. Sahni, C. V. Tomy, G. Balakrishnan, D. Mck. Paul, and S. Bhattacharya, *Physica C* **256**, 119 (1996); S. Ramakrishnan, N. G. Patil, S. S. Banerjee, Subir Saha, K. Ghosh, A. K. Grover, Gautam I. Menon, P. K. Mishra, T. V. Chandrasekhar Rao, G. Ravikumar, V. C. Sahni, C. V. Tomy, G. Balakrishnan, D. Mck. Paul, and S. Bhattacharya, *Czech. J. Phys.* **46**, 3105 (1996).
- ²²C. P. Bean, *Rev. Mod. Phys.* **36**, 31 (1964); X. S. Ling and J. Budnick, in *Magnetic Susceptibility of Superconductors and other Spin Systems*, edited by R. A. Hein, T. L. Francavilla, and D. H. Leibenberg (Plenum Press, New York, 1991), p. 377.
- ²³L. A. Angurel, F. Amin, M. Polichetti, J. Aarts, and P. H. Kes, *Phys. Rev. B* **56**, 3425 (1997) and references cited therein.
- ²⁴G. Ravikumar, T. V. C. Rao, P. K. Mishra, V. C. Sahni, Subir Saha, S. S. Banerjee, N. G. Patil, A. K. Grover, S. Ramakrishnan, S. Bhattacharya, E. Yamamoto, Y. Haga, M. Hedo, Y. Inada, and Y. Onuki, *Physica C* **276**, 9 (1997); **298**, 122 (1998).
- ²⁵A. Durate, E. F. Righi, C. A. Bolle, F. de la Cruz, P. L. Gammel, C. S. Oglesby, E. Bucher, B. Batlogg, and D. J. Bishop, *Phys. Rev. B* **53**, 11 336 (1996).
- ²⁶M. V. Marchevsky, Ph.D. thesis, University of Leiden, The Netherlands, 1997, Chap. 4.
- ²⁷A. I. Larkin, *Zh. Éksp. Teor. Fiz.* **58**, 1466 (1970) [*Sov. Phys. JETP* **31**, 784 (1970)]; A. I. Larkin and Yu. N. Ovchinnikov, *J. Low Temp. Phys.* **34**, 409 (1979).
- ²⁸R. Wördenweber and P. H. Kes, *Phys. Rev. B* **34**, 494 (1986), and references therein.
- ²⁹S. S. Banerjee, Ph.D. thesis, University of Mumbai, India, 2000.
- ³⁰Y. Paltiel, D. T. Fuchs, E. Zeldov, Y. N. Myasoedov, H. Shtrikman, M. L. Rappaport, and E. Y. Andrei, *Phys. Rev. B* **58**, R14 763 (1998).